Electronic Transport, Structure, and Energetics of Endohedral Gd@C$_{82}$ Metallofullerenes

L. Senapati, J. Schrier,* and K. B. Whaley

Department of Chemistry and Pitzer Center for Theoretical Chemistry, University of California, Berkeley, California 94720-1460

ABSTRACT

Electronic structure and transport properties of the fullerene C$_{82}$ and the metallofullerene Gd@C$_{82}$ are investigated with density functional theory and the Landauer−Büttiker formalism. The ground-state structure of Gd@C$_{82}$ is found to have the Gd atom below the C−C bond on the C$_2$ molecular axis of C$_{82}$. Insertion of Gd into C$_{82}$ deforms the carbon chain in the vicinity of the Gd atoms. Significant overlap of the electron distribution is found between Gd and the C$_{82}$ cage, with the transferred Gd electron density localized mainly on the nearest carbon atoms. This charge localization reduces some of the conducting channels for the transport, causing a reduction in the conductivity of the Gd@C$_{82}$ species relative to the empty C$_{82}$ molecule. The electron transport across the metallofullerene is found to be insensitive to the spin state of the Gd atom.

I. Introduction. Endohedral metallofullerences[1] have attracted wide interest due to their functional characteristics and potential applications in the fields of nanomaterials and biomedical science.[2] Recently, metallofullerene-doped nanotubes ("peapods") have also attracted experimental attention due to their structural and electronic properties[3−5] and have been proposed as a possible self-assembled quantum computing architecture.[6] Additionally, recent experimental studies of Gd@C$_{82}$ in single-walled carbon nanotube ((Gd@C$_{82}$)@SWNT) peapods have shown novel transport behavior.[7] The first step in understanding the properties of the peapod structures is an adequate treatment of the individual Gd@C$_{82}$ fullerenes.

In earlier Gd@C$_{82}$ theoretical calculations by Kobayashi and Nagase,[8] neither the relaxation of the fullerene cage nor the possibility of novel geometries for the Gd atom in the fullerene cage was considered; the predicted ground-state spin multiplicity M=9, resulting from ferromanetic coupling between the Gd f-electrons and the odd electron on the fullerene cage, is in contrast to electron spin resonance determinations of an M=7 ground state, due to antiferromagnetic coupling of −1.8 cm^{-1}.[9] The M=7 ground state is also supported by magnetic studies.[10−13] To resolve this discrepancy, we present results of density functional calculations for the equilibrium geometries and magnetic and transport properties of Gd@C$_{82}$, made with the Landauer−Buttiker transport formalism. Section II gives a brief description of the theoretical procedure, Section III presents our

results, and Section IV draws conclusions and discusses possible future directions.

II. Computational Methods. The equilibrium geometry and the total energy of Gd@C$_{82}$ are calculated using density functional theory (DFT).[14] One of the primary considerations involved in these calculations is determination of a suitable basis set and exchange correlation functional. We therefore compared the bond length, binding energy, and spin multiplicity values of Gd and Gd dimer (Gd$_2$) optimized using several different basis sets and exchange correlation functionals to experimental values[15] and theoretical all-electron relativistic calculations.[16] As we discuss in Section IIIA, the results are quite sensitive to the choices of both basis set and exchange correlation functional. A relativistic effective core potential CEP-121G[17] for the atoms with the generalized gradient approximation of Becke's exchange functional[18] and Lee−Yang−Parr correlational functional[19] (B3LYP) gave results comparable to experiment and were thus used for the subsequent calculations.

The total energies and forces are calculated using the linear combination of atomic orbitals (LCAO) molecular orbital approach.[14] We employed a 6-31G basis set for the carbon atoms and a CEP-121G basis set for Gd. The computations were performed using Gaussian 03 for various spin multiplicities.[20] The geometries were optimized without symmetry constraints by minimizing the total energy and requiring the forces to vanish within a 10^{-3} a.u./Bohr threshold, at every atom site. To find the ground state structure for Gd@C$_{82}$, initial positions of the Gd atom inside the C$_{82}$ cage were generated then optimized without constraining any of the

---

* Corresponding author. E-mail: jschrier@berkeley.edu.
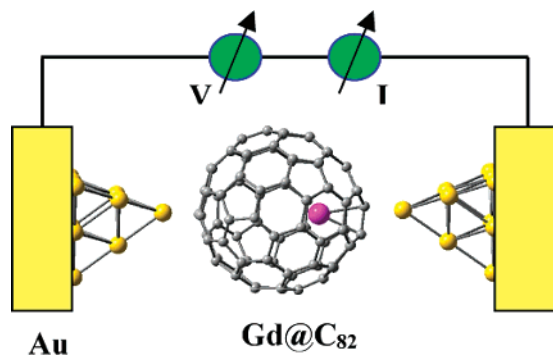
Figure 1. Gold contact model used for transport calculations across Gd@C_{82}. The first layer adjacent to C_{82} has one Au atom, the second has three Au atoms, and the third layer has six Au atoms.

atomic coordinates. The calculations were repeated for different spin multiplicities to determine the ground state spin configuration, as we discuss in Section IIIB. Although the partitioning of charge to specific atoms or groups within a molecule is not uniquely defined within the postulates of quantum mechanics,[21] a recent experimental evaluation of density functional charge schemes[22] found the commonly used Mulliken charge analysis[21] to be generally deficient for charge calculations and found natural population analysis[23] (NPA) to be the most generally accurate method of those studied.

To study the transport, we created a model composed of C_{82} located between two Au contacts, with and without the endohedral Gd atom. The numbers of Au atoms on each side of the contact were varied to study the transport dependence on contact geometry. Figure 1 shows one of these structures with a triangular contact of three Au layers in which the layer adjacent to C_{82} has one Au atom, the second has three Au atoms, and the third layer has six Au atoms. For calculation of electron transport through Gd@C_{82} and C_{82}, we used the nonequilibrium Green's function based Landauer−Büttiker formalism.[24−26] Neglecting spin-flip processes, the total current due to coherent scattering is given by $I_{spin-coherent} = I^{\alpha} + I^{\beta}$, where I^{α} and I^{β} are the contribution to current from spin up (α) and down (β) states, respectively. The spin specific contributions are expressed as the integral over the injection energy of the tunneling electron, E,

$$I^{\alpha(\beta)} = (e/h) \int_{\mu_2}^{\mu_1} T^{\alpha(\beta)}(E,V)[f(E,\mu_1) - f(E,\mu_2)] \, dE \quad (1)$$

taken between the electrochemical potentials μ_1 and μ_2,

$$\mu_1 = E_F - (q_1 V/(q_1 + q_2)) \quad (2)$$

$$\mu_2 = E_F + (q_2 V/(q_1 + q_2)) \quad (3)$$

where q_1 and q_2 are charge accumulated in the left and right contacts, respectively, V is the applied bias, and E_F is the Fermi energy of the gold contact, taken as -5.53 eV for our calculation. The term $f(E,\mu)$ is the Fermi distribution function and $T^{\alpha(\beta)}(E, V)$ is the transmission function that represents the sum of transmission probabilities for electrons

of a given spin through the contact/metallofullerene complex, obtained from the overlap and Hamiltonian matrices determined by the DFT calculation. The explicity included Au atoms in our model system described above are used to obtain the coupling matrices for calculation of self-energy functions.[24,26] We have used the local density of states of the 6s-band of bulk gold (0.035 eV per electron spin) to approximate the Green's function of the (bulk) Au contact.[26]

III. Results. *A. Properties of Gd and Gd_2.* First, we discuss the geometry, ionization potential, and electron affinity of Gd and Gd_2 and compare these with experiment. This comparison is provided to assess the accuracy of our theoretical procedure.

To assess how well our method accounts for the properties of the Gd atom, we have calculated the ionization potential of Gd and Gd_2 as well as the binding energy and Gd_2 dimer bond length. The ground-state Gd atom was found to have a spin multiplicity of 9 for all functionals that we have considered with the CEP-121G effective core potential basis functions.[17] Results for the LSDA,[14] B3LYP,[18,19] and PW91[27] functionals are presented in supplemental Table 1 (see Supporting Information). The calculated binding energy value (1.7595 eV) and bond length (2.926 Å) for Gd_2 with CEP-121G as frozen core basis function and B3LYP as functional for spin multiplicity of 19 agrees well with the experimental binding energy (1.784 ± 0.35 eV)[15] and the relativistic all-electron theoretical bond-length (2.895 Å).[16] The ionization potential for Gd and Gd_2 were calculated as 5.014 and 4.119 eV respectively. Based on these results, the CEP-121G basis set for Gd and 6-31G basis set for C atoms, together with the B3LYP functional, were used for the Gd@C_{82} calculations.

Although we have employed a frozen core, the Gd 5s and 5p core electrons are allowed to relax in the molecular calculations. Atomic calculations show that the relaxation of these states is often crucial for an accurate determination of valence state properties because of the overlap of the 5d electron orbitals with the other $n=5$ orbitals.

B. Structure of Gd@C_{82}. We have taken a C_{82} fullerene cage with C_{2v} point group symmetry $C_{82}(C_{2v})$ and optimized the structure with Gd inside at various positions, as described in Section II. In the $C_{82}(C_{2v})$ fullerene cage, the C_2 axis goes through the center of one six-membered ring and one C−C double bond. Our calculations reveal that the ground-state structure of Gd@C_{82} has the Gd atom situated adjacent to the C−C double bond on the symmetry axis, as shown in Figure 2. This is in contrast to reported results for other metal atoms such as Sc, Y, and La in C_{82},[8,28−32] where the metal atoms are found to be centered inside the fullerene cage on top of the C_{2v} axis six-membered ring.[8,29] Recent synchrotron radiation powder structure analysis experiments of Gd@C_{82} are consistent with our calculated placement of the Gd atom.[33] The distances between Gd and the two nearest C atoms are 2.38 and 2.41 Å, respectively. The binding energy of Gd to C_{82} is found to be 5.6435 eV (130.1 kcal/mol), comparable to those for the Sc, Y, and La metallofullerenes;[8] the energy levels of C_{82} and Gd@C_{82} are shown in supplemental Figure 1 (Supporting Information). Addition of Gd into C_{82} slightly lengthens the proximal C−C bond
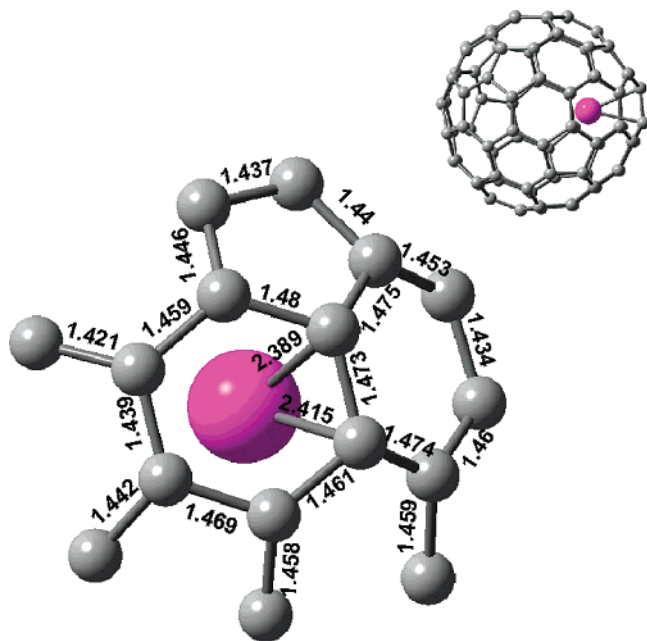
Figure 2. Optimized structure of Gd@C_{82}. The ground-state structure of Gd@C_{82} has the Gd atom (purple) situated adjacent to the C–C double bond on the C_{2v} symmetry axis that connects a six-membered ring with a C=C bond on the other side of the fullerene. The distances between Gd and the two nearest C atoms are 2.38 and 2.41 Å, respectively. The lines between Gd and C are used to indicate the closest carbon atoms.

(from 1.425 to 1.473 Å) atom, as well as the neighboring C–C bonds (by 0.01 to 0.04 Å). This deformation results in an energy difference between the $C_{82}(C_{2v})$ symmetry structure and the Gd@C_{82} optimized deformed structure when recalculated without Gd of 0.109 eV (2.51 kcal/mol).

As discussed in Section II, the NPA charge partitioning tends to give better results; our Gd@C_{82} calculations agree with this analysis, as the Mulliken charge analysis indicates charge transfer of 1.43 electrons from Gd atom to the C_{82} cage, and NPA indicates a charge transfer of 2.43 electrons. The latter value agrees well with electron energy loss spectroscopy (EELS) experiments.[34] The electrons are localized near the two proximal carbon atoms, resulting in strong charge density overlap between the Gd atom and these C atoms. NPA analysis also gives a Gd d-orbital population of 0.48 electrons, consistent with a Dewar–Chatt backbonding interaction between the Gd atom and the carbon double bond.[35] The deformation of the C–C bonds near the Gd is also consistent with back-bonding, as the back-donation of charge from the C–C bonds to the d-orbitals weakens (and hence lengthens) the bonds. Additionally, the Gd f-orbital population of 7.02 is consistent with the charge transfer from the cage of 0.04 electrons empirically determined by Nadaï et al. for reproducing X-ray magnetic circular dichroism experiments.[36]

To study the difference in Gd placement, as compared to the Sc, Y, and La cases, we performed single-point calculations, in which the Gd atom was placed in the La-like position, adjusting the distance between the hexagon and the Gd atom to account for the smaller radius of the Gd^{3+} ion as compared to the La^{3+} ion.[37] The lowest total energy

structure we found occurred when the Gd atom was placed 2.10 Å above the plane of the hexagon; this structure had a total energy of 0.104 hartrees (2.83 eV) higher than the ground position determined by our optimizations. NPA analysis determined nearly identical charge distribution on the Gd atom in both cases, attesting to the importance of Gd–C back-bonding in stabilizing the structure. However, an elementary electrostatic analysis, using the NPA atomic charges as point ions, gives a Gd-cage potential energy of −1.015 and −0.9366 hartrees for the ground and La-like positions, respectively; the difference between these nearly accounts for the difference in total energies. This interpretation is consistent with resonant photoemission spectroscopy experiments which suggest that the Gd–C bond is primarily ionic in character.[38]

We have also examined the effect of different spin configurations on the optimized Gd@C_{82} structure. The ground-state structure was found to have seven unpaired electrons on Gd and one unpaired electron on the C_{82} cage aligned antiparallel to the Gd spins, with total spin multiplicity M=7, in agreement with magnetic studies.[10–13] The next lowest energy structure has M=9, with seven unpaired electrons at Gd and the odd C_{82} cage electron oriented parallel to the Gd spins. The energy difference between these two configurations is 2.6 meV (16.1 cm^{-1}), which compares favorably to the experimentally determined value of 14.4 cm^{-1}.[9] The detailed energies with various spin multiplicities are listed in Table 1.

Table 1. Calculated Total Energies and Binding Energies for the Optimized Structures of C_{82} and Gd@C_{82} as a Function of Gd Spin Multiplicity, M[a]

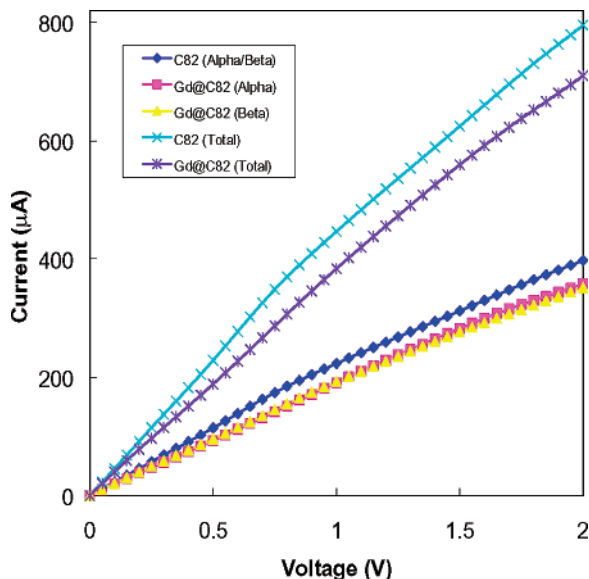| Atom (M)	TE (au)	B(eV)
$C_{82}(C_{2v})$	−3123.805927	
Gd@C_{82}(M=5)	−3235.8783289	4.4066
Gd@C_{82}(M=7)	−3235.9237819	5.6435
Gd@C_{82}(M=9)	−3235.9236904	5.6409
Gd@C_{82}(M=11)	−3235.87890696	4.4224

[a] The M=7 state of Gd@C_{82} is found to be 2.6 meV below the M=9 state in total energy.

C. Electronic Transport. To see the effects of contact geometry, we have taken between one and three layers of Au atoms to represent the contact. To obtain the contacts, single Au atoms were placed on each side of the Gd@C_{82} molecule, shown schematically in Figure 1, at a distance of 2.015 Å from the carbon atoms, along the C_{2v} symmetry axis. To build the larger contacts, the bond lengths and geometry of bulk Au were used to add three Au atoms to the second layer and six Au atoms to the third layer, as shown in Figure 1. Although it is known that the conductance can be strongly dependent on the contact structure,[39] this transport model serves as the basis for understanding the qualitative transport properties of Gd@C_{82}.

Calculated $I-V$ characteristics for C_{82} and Gd@C_{82} with various spin states and Au contact geometries are shown in Figures 3−5 and supplemental Figure 3 (Supporting Information). The ground state (M=7) transport with a single Au
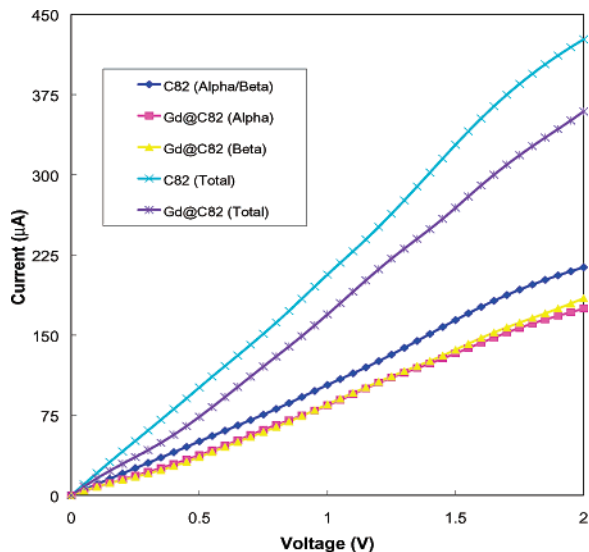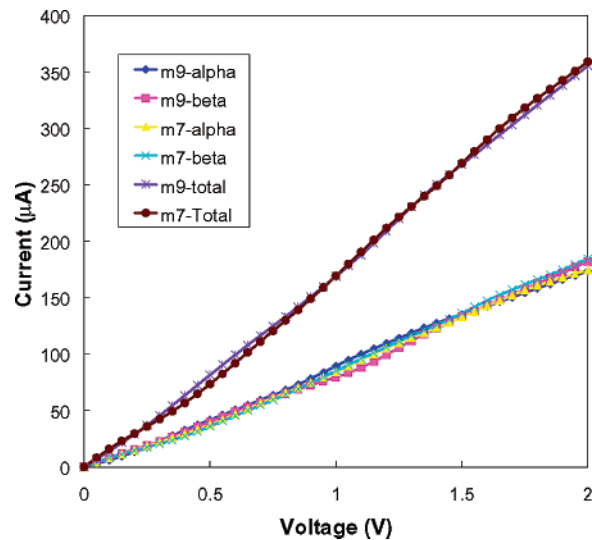
Figure 3. *I−V* plot for single Au atom contacts. Total conduction (sum of spin up and spin down conduction) for Gd@C$_{82}$ is lower at all bias voltages than for pure fullerene C$_{82}$. Conduction of spin up (alpha) and spin down (beta) electrons is similar at all bias values.

Figure 5. *I−V* plot for conduction in the spin multiplicity M=7 ground state, and the M=9 state with energy 2.6 meV higher in energy. Conduction characteristics for spin polarized and unpolarized currents are similar for both cases, with neither showing strong spin-dependent transport effects. This suggests that the current is mainly carried through the C$_{82}$ cage and does not involve the Gd atom.
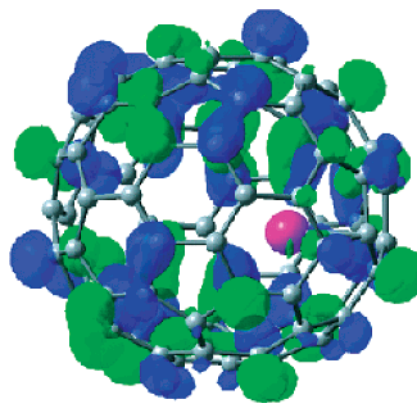

Figure 4. *I−V* plot for contact geometry shown in Figure 1. Note the qualitative similarity to the other contact geometries (Fig. 3 and supplemental Figure 2).

Figure 6. Lowest unoccupied molecular orbital (LUMO) plot of Gd@C$_{82}$ showing localization on the C$_{82}$ cage without significant LUMO orbitals on the Gd atom. Blue and green are used to indicate the positive and negative sign of the wave function, respectively. The purple sphere indicated the Gd atom.

atom contact on each side of the fullerene is shown in Figure 3. Addition of the Gd atom into the C$_{82}$ cage leads to a reduction in the current. To understand this difference, we computed the density of state (DOS) for both structures and found the metallofullerene to have a reduced DOS near the Fermi energy as compared to C$_{82}$. These results are shown in supplemental Figure 2 (Supporting Information). The *I−V* characteristics for the two- and three-layer contact structures were found to be qualitatively the same as for the single Au atom contact case and are shown in supplemental Figure 3 (Supporting Information) and Figure 4, respectively. Quantitatively, the current is seen to increase with the addition of more gold layers, due to the increasing number of conduction channels.

Calculations for the M=9 structure, which is structurally degenerate to the M=7 system, are shown in Figure 5. We find only a small difference in current between the two spin configurations, and the conduction properties of spin up and spin down electrons (as calculated in eq 1) were found to be insensitive to the Gd spin configurations, suggesting that the spin of the Gd is shielded by the cage carbon atoms and that transport occurs consequently only through the fullerene cage. This is also supported by plots of the highest occupied and lowest unoccupied molecular orbitals (HOMO/LUMO), shown in Figures 6 and 7, which indicate that conduction occurs primarily through the C$_{82}$ cage and shows no signature of conducting paths involving the Gd atom. This suggests that incorporation of Gd decreases the number of available conduction channels between the contacts, as a result of the charge localization effect noted in Section IIIB.
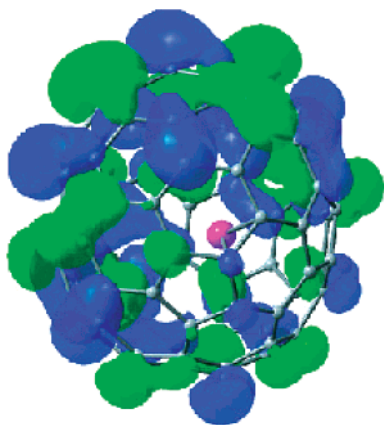
Figure 7. Highest occupied molecular orbital (HOMO) plot of $Gd@C_{82}$. Blue and green are used to indicate the positive and negative sign of the wave function. HOMO orbitals are localized on cage of C_{82} and there is no HOMO orbital on Gd (purple sphere). From both HOMO and LUMO plots, it is evident that the current is mainly carried through the C_{82} cage, as opposed to the Gd atom.

By attaching the Au contacts, one expects some charge transfer from the metallic contact to the fullerene at zero bias, but this effect (which is the same for both structures) is relatively small due to the weak coupling between the fullerene and metal contact. Using the NPA method described in the previous section, the charge transfers from the left and right Au contacts to the C_{82} cage were found to be 0.09 and 0.11 electrons for a single layer of Au, 0.12 and 0.13 electrons for the two-layer contact, and 0.13 and 0.15 electrons for the three-layer contact. Use of these charge values in the expression for the electrochemical potential, eq 2, had no effect on the calculated transport properties. Despite the fact that Gd is closer to one of the electrodes, we observed no diode like behavior; we attribute this to the conduction occurring primarily through the fullerene cage, which is approximately symmetrical with respect to both contacts.

IV. Conclusions. We have analyzed the energetics, structure, and transport properties of $Gd@C_{82}$. The present results indicate that the CEP-121G basis set for Gd, with the B3LYP density functional for exchange and correlation, is a satisfactory combination for DFT calculations for large Gd endofullerene systems. Our calculated structure for $Gd@C_{82}$ confirms the geometry determined by X-ray diffraction data, indicating that the Gd is located adjacent to the C−C double bond on the symmetry axis, in contrast to the other Group 3 metallofullerenes. Furthermore, this geometry gives calculated spin configurations that agree with ESR and magnetic experiments, in contrast to previous theoretical studies. Using the Landauer−Büttiker formalism for transport, we find that conduction occurs primarily through the C_{82} cage and that charge donation from the Gd atom to the cage disrupts these conduction channels. We find no evidence for electron-spin dependent transport effects due to the spin state of the Gd atom. Besides providing a solid methodological and structural basis for future calculations of $(Gd@C_{82})@SWNT$ structures, the absence of HOMO/LUMO density on the Gd atom−and thus relative lack of interaction with the surrounding nanotube−helps explain why

the M_4 and M_5 peak edges of the $(Gd@C_{82})@SWNT$ EELS spectrum were found to be identical to that for $Gd@C_{82}$, indicating that the Gd valence state is unaffected by the surrounding nanotube.[7]

Supporting Information Available: Results for the LSDA, B3LYP, and PW91 functionals (Table 1); energy levels of C_{82} and $Gd@C_{82}$ (Figure 1); density of states (Figure 2), and calculated $I-V$ characteristics for C_{82} and $Gd@C_{82}$ with various spin states and Au contact geometries (Figure 3). This material is available free of charge via the Internet at http://pubs.acs.org.

References

(1) Shinohara, H. *Rep. Prog. Phys.* **2000**, *63*, 843.
(2) Bethune, D.; Johnson, R.; Salem, J. R.; Vries, M.; Yannoni, C. *Nature* **1993**, *366*, 123.
(3) Lee, J.; Kim, H.; Kahng, S.-J.; Kim, G.; Son, Y.-W.; Ihm, J.; Kato, H.; Wang, Z. W.; Okazaki, T.; Shinohara, H.; et al. *Nature* **2002**, *415*, 1005.
(4) Hirahara, K.; Suenaga, K.; Bandow, S.; Kato, H.; Okazaki, T.; Shinohara, H.; Iijima, S. *Phys. Rev. Lett.* **2002**, *85*, 5384.
(5) Shimada, T.; Okazaki, T.; Taniguchi, R.; Sugai, T.; Shinohara, H.; Suenaga, K.; Ohno, Y.; Mizuno, S.; Kishimoto, S.; Mizutani, T. *Appl. Phys. Lett.* **2002**, *81*, 4067.
(6) Ardavan, A.; Austwick, M.; Benjamin, S.; Briggs, G.; Dennis, T. J. S.; Ferguson, A.; Hasko, D. G.; Kanai, M.; Khlobystov, A.; Lovett, B.; et al., *Philos. Trans. Roy Soc. London A* **2003**, *361*, 1473.
(7) Okazaki, T.; Shimada, T.; Suenaga, K.; Ohno, Y.; Mizutani, T.; Lee, J.; Kuk, Y.; Shinohara, H. *Appl. Phys. A* **2003**, *76*, 475.
(8) Kobayashi, K.; Nagase, S. *Chem. Phys. Lett.* **1998**, *282*, 325.
(9) Furukawa, K.; Okubo, S.; Kato, H.; Shinohara, H.; Kato, T. *J. Phys. Chem. A* **2003**, *107*, 10933.
(10) Funasaka, H.; Sakurai, K.; Oda, Y.; Yamamoto, K.; Takahashi, T. *Chem. Phys. Lett.* **1995**, *232*, 273.
(11) Funasaka, H.; Sugiyama, K.; Yamamoto, K.; Takahashi, T. *J. Phys. Chem.* **1995**, *99*, 1826.
(12) Huang, H. J.; Yang, S. H.; Zhang, X. X. *J. Phys. Chem. B* **1999**, *103*, 5928.
(13) Huang, H.; Yang, S.; Zhang, X. *J. Phys. Chem. B* **2000**, *104*, 1473.
(14) Parr, R. G.; Yang, W. *Density-Functional Theory of Atoms and Molecules*; Oxford Science: Oxford, 1994.
(15) Kant, A.; Lin, S. S. *Monash. Chem.* **1971**, *103*, 757.
(16) Dolg, M.; Liu, W.; Kalvoda, S. *Int. J. Quantum Chem.* **2000**, *76*, 359.
(17) Cundari, T. R.; Stevens, W. J. *J. Chem. Phys.* **1993**, *98*, 5555.
(18) Becke, A. D.; *J. Chem. Phys.* **1993**, *98*, 5648.
(19) Lee, C.; Yang, W.; Parr, R. G. *Phys. Rev. B* **1988**, *37*, 785.
(20) Frisch, M. J.; Trucks, G. W.; Schlegel, H. B.; Scuseria, G. E.; Robb, M. A.; Cheeseman, J. R.; Montgomery, J. A., Jr.; Vreven, T.; Kudin, K. N.; Burant, J. C.; Millam, J. M.; Iyengar, S. S.; Tomasi, J.; Barone, V.; Mennucci, B.; Cossi, M.; Scalmani, G.; Rega, N.; Petersson, G. A.; Nakatsuji, H.; Hada, M.; Ehara, M.; Toyota, K.; Fukuda, R.; Hasegawa, J.; Ishida, M.; Nakajima, T.; Honda, Y.; Kitao, O.; Nakai, H.; Klene, M.; Li, X.; Knox, J. E.; Hratchian, H. P.; Cross, J. B.; Adamo, C.; Jaramillo, J.; Gomperts, R.; Stratmann, R. E.; Yazyev, O.; Austin, A. J.; Cammi, R.; Pomelli, C.; Ochterski, J. W.; Ayala,

P. Y.; Morokuma, K.; Voth, G. A.; Salvador, P.; Dannenberg, J. J.; Zakrzewski, V. G.; Dapprich, S.; Daniels, A. D.; Strain, M. C.; Farkas, O.; Malick, D. K.; Rabuck, A. D.; Raghavachari, K.; Foresman, J. B.; Ortiz, J. V.; Cui, Q.; Baboul, A. G.; Clifford, S.; Cioslowski, J.; Stefanov, B. B.; Liu, G.; Liashenko, A.; Piskorz, P.; Komaromi, I.; Martin, R. L.; Fox, D. J.; Keith, T.; Al-Laham, M. A.; Peng, C. Y.; Nanayakkara, A.; Challacombe, M.; Gill, P. M. W.; Johnson, B.; Chen, W.; Wong, M. W.; Gonzalez, C.; Pople, J. A. *Gaussian 03*, Gaussian, Inc.: Pittsburgh, PA, 2003.

(21) Szabo, A.; Ostlund, N. S. *Modern Quantum Chemistry*; Dover: Mineola, NY, 1996.

(22) Yerulshalmi, R.; Scherz, A.; Baldridge, K. K. *J. Am. Chem. Soc.* **2004**, *126*, 5897.

(23) Reed, A. E.; Weinstock, R. B.; Weinhold, F. *J. Chem. Phys.* **1985**, *83*, 735.

(24) Datta, S. *Electron Transport in Mesoscopic Systems*; Cambridge University Press: Cambridge, 1997.

(25) Pati, R.; Senapati, L.; Ajayan, P. M.; Nayak, S. K. *Phys. Rev. B* **2003**, *68*, 100407.

(26) Tian, W.; Datta, S.; Hong, S.; Reifenberger, R.; Henderson, J. I.; Kubiak, C. P. *J. Chem. Phys.* **1998**, *109*, 2874.

(27) Perdew, J. P.; Wang, Y. *Phys. Rev. B* **1992**, *45*, 13244.

(28) Takata, M.; Umeda, B.; Nishibori, E.; Sakata, M.; Saito, Y.; Ohno, M.; Shinohara, H. *Nature* **1995**, *377*, 46.

(29) Nishihori, E.; Takata, M.; Sakata, M.; Tanaka, H.; Hasegawa, M.; Shinohara, H. *Chem. Phys. Lett.* **2000**, *330*, 497.

(30) Nishihori, E.; Takata, M.; Sakata, M.; Inakuma, M.; Shinohara, H. *Chem. Phys. Lett.* **1998**, *298*, 79.

(31) Kobayashi, K.; Nagase, S. In *Endohedralfullerenes: A New Family of Carbon Clusters*; Akasaka, T., Nagase, S., Eds.; Kluwer: Dordrecht, 2002; pp 99−119.

(32) Kobayashi, K.; Nagase, S. *Mol. Phys.* **2003**, *101*, 249.

(33) Nishibori, E.; Iwata, K.; Sakata, M.; Takata, M.; Tanaka, H.; Kato, H.; Shinohara, H. *Phys. Rev. B* **2004**, *69*, 113412.

(34) Suenaga, K.; Iijima, S.; Kato, H.; Shinohara, H. *Phys. Rev. B* **2000**, *62*, 1627.

(35) Crabtree, R. H. *The Organometallic Chemistry of the Transition Metals*, 2nd ed; Wiley-Interscience: New York, 1994.

(36) Nadaï, C. D.; Mirone, A.; Dhesi, S. S.; Bencok, P.; Brookes, N. B.; Marenne, I.; Rudolf, P.; Tagmatarchis, N.; Shinohara, H.; Dennis, T. J. S.; *Phys. Rev. B* **2004**, *69*, 184421.

(37) Cotton, F. A.; Wilkinson, G.; Murillo, C. A.; Bochmann, M. *Advanced Inorganic Chemistry*, 6th ed.; Wiley-Interscience: New York, 1999.

(38) Pagliara, S.; Sangaletti, L.; Cepek, C.; Bondino, F.; Larciprete, R.; Goldoni, A. *Phys. Rev. B* **2004**, *70*, 035420.

(39) Ke, S.-H.; Baranger, H. U.; Yang, W. cond-mat/0402409.

NL049164U